Microscopy and Microanalysis (2020), 1–8
doi:10.1017/S1431927620024319

Microscopy AND Microanalysis

Micrographia

A Novel Method Using Confocal Laser Scanning Microscopy for Three-Dimensional Analysis of Human Dental Enamel Subjected to Ceramic Bracket Debonding

Fabiano G. Ferreira[1]*, Eduardo M. da Silva[2] and Oswaldo de V. Vilella[1]

[1]Department of Orthodontics, School of Dentistry, Universidade Federal Fluminense, Niterói, Rio de Janeiro 24020-140, Brazil and [2]Analitical Laboratory of Restorative Biomaterials – LABiom-R, School of Dentistry, Universidade Federal Fluminense, Niterói, Rio de Janeiro 24020-140, Brazil

Abstract

The aim of this *in vitro* study was to present a method using confocal laser scanning microscopy for three-dimensional analysis of human dental enamel subjected to ceramic bracket debonding. The labial enamel surfaces of three upper central incisors were prepared and mounted in the form of standardized specimens. A sample repositioning protocol was established to enable surface measurement and analysis before and after bracket debonding. Observations were made of representative areas measuring 1,280 × 1,280 μm^2, in the center of the enamel samples, as well as of the total topography (2,500 × 3,500 μm) of the bonding areas provided by the equipment software. Noncontact three-dimensional high-resolution image analyses revealed the capabilities of the employed technique and methodology to permit the examination of specific characteristics and alterations on the surfaces, before and after the debonding and finishing procedures. The new protocol was effective to provide qualitative and quantitative assessments of changes on the same dental surfaces at different trial times. The methodology constitutes a feasible tool for revealing the effects of debonding of ceramic brackets on sound and previously injured dental enamel surfaces.

Key words: bracket debonding, confocal laser scanning microscopy, dental enamel, microscopy, surface analysis

(Received 10 March 2020; revised 22 July 2020; accepted 3 August 2020)

Introduction

Orthodontic appliance debonding followed by finishing procedures to remove resin remnants from enamel surfaces should restore the original esthetics and contours, while minimizing iatrogenic effects such as wear and loss of the substrate (Campbell, 1995). Nevertheless, the removal of fixed orthodontic appliances can cause irreversible damage to tooth surfaces, in the form of cracks or enamel fractures (Cochrane et al., 2017).

Previous studies revealed an association between the ceramic bracket debonding process and increases in the length (Heravi et al., 2008; Dumbryte et al., 2016, 2017) and width (Dumbryte et al., 2016, 2017) of enamel microcracks. Recently, a systematic review pointed out that although quantitative studies show weak evidence because of the lacking of parameter number analysis, there is strong evidence for the increasing of the enamel microcracks after debonding (Dumbryte et al., 2018). Previous work reported that resin-enamel bond strength values between 5.9 and 7.8 MPa are required to maintain brackets fixed to enamel surfaces (Reynolds, 1975). However, the higher bonding strength of the ceramic bracket base, compared to that of a metal bracket, and the higher bond strength values of the bonding systems involving the enamel, the adhesive, and the bracket, increase the risk of enamel damage on debonding (Gwinnett, 1988; Bishara et al., 2002). It occurs because these values exceed the cohesive strength of enamel, consequently producing cracks and fractures more easily (Rix et al., 2001) and increasing the possibility of substrate loss at the time of debonding (Powers et al., 1997).

Different methods have been used to evaluate the presence of changes in the enamel structure after ceramic bracket removal and enamel surface finishing. Among the most commonly used techniques, scanning electron microscopy (SEM) is highlighted for providing qualitative analysis of the injuries caused to the tooth (Dumbryte et al., 2016). However, drawbacks of SEM include issues related to two-dimensional image reproduction, the possibility of causing destructive alteration of the sample surface during the preparation process, and the need for specific environmental conditions during the analysis (Field et al., 2010). In addition, on its own, this method is unable to provide quantitative surface information (Karan et al., 2010). Alternatively, three-dimensional techniques such as optical coherence tomography (OCT) have recently been considered as useful tools for effective measurement of the entire volume of the enamel layer, before and after the debonding of ceramic brackets (Leão Filho et al., 2015; Machoy et al., 2019). However, no reports have yet described a protocol for mapping the entire surface of

*Author for correspondence: Fabiano Guerra Ferreira, E-mail: drfabianoguerra@ig.com.br

Cite this article: Ferreira FG, da Silva EM, Vilella OdeV (2020) A Novel Method Using Confocal Laser Scanning Microscopy for Three-Dimensional Analysis of Human Dental Enamel Subjected to Ceramic Bracket Debonding. *Microsc Microanal.* doi:10.1017/S1431927620024319

the bonding area or have provided data relating how a specific surface irregularity or injury may influence the analysis of the entire surface, after different testing conditions.

The methodology for sample evaluation at different times or stages of a treatment has also been discussed. A previous work pointed out that, although a number of studies have compared treated and nontreated groups, they had not confirmed whether the surfaces were undamaged before the brackets were bonded, or have considered whether the surface treatment applied to the enamel might hinder damage detection (Kitahara-Céia et al., 2008). Considering the tooth enamel presents nonflat and heterogeneous surface topography, with inherently variable structural characteristics (Gutiérrez-Salazar & Reyes-Gasga, 2003; Ferreira et al., 2014), comparisons performed using different dental surfaces could preclude precise detection of damage caused by the removal and finishing procedures (Kitahara-Céia et al., 2008).

Moreover, some techniques concerning the examination of the same dental enamel surfaces before and after ceramic bracket debonding have not described protocols to ensure that the analyses were performed at the same specific areas (Habibi et al., 2007; Bishara et al., 2008; Ahrari et al., 2012). Nevertheless, recent studies have proposed a method to quantitatively measure crack characteristics (visibility, direction, location, length, and width) in specific surface sites, before and after ceramic bracket debonding, employing SEM (Dumbryte et al., 2015, 2017). The authors concluded the technique might enable precise detection as well as the prediction of the presence of enamel microcracks even before the beginning of the orthodontic treatment.

The development of new hardware and software technologies capable of providing three-dimensional images has enabled the precise and repeatable characterization of the same large areas of the enamel surface, before and after metallic bracket debonding (Ferreira et al., 2014). The characterization of the surface could be achieved, regardless of the substrate topography, using a noncontact three-dimensional optical profilometry technique (Ferreira et al., 2014).

Considering the above mentioned, the aim of this *in vitro* pilot study was to present a method for three-dimensional qualitative and quantitative analysis of changes on dental surfaces submitted to ceramic bracket debonding, using, for the first time, confocal laser scanning microscopy (CLSM). Significant surface areas measuring $1{,}280 \times 1{,}280\ \mu m^2$ and panoramic assessments of the total bracket areas on the enamel samples were performed before bonding and after the removal of resin remnants from the surfaces.

Materials and Methods

This pilot study was part of a broader postdoctoral research program. The project was approved by the Research Ethics Committee of Universidade Federal Fluminense (Niterói, Rio de Janeiro, Brazil) and was registered under the protocol number CAAE 17558119.8.0000.5243.

The teeth used were donated by the tooth bank of Universidade Federal de Juíz de Fora (Juíz de Fora, Minas Gerais, Brazil) and were prepared and mounted according to international standards (ISO/TS 11405:2003).

The experiment employed three maxillary central incisors that had been freshly extracted for periodontal purposes. The criteria for tooth selection were as follows: (sample 1) tooth with the absence of damage caused by the extraction process and no white spot lesions, caries, or restorations; (sample 2) tooth showing the presence of at least one erosion area and scratches on the surface; (sample 3) tooth showing the presence of areas of erosion and microcracks on the surface. These topographic features were identified using a stereomicroscope (Model EK3ST, CQA, Paulínia, São Paulo, Brazil), at ×20 on scope magnification.

Sample Preparation

A standardized protocol modified from Ferreira et al. (2014) was established for preparation and precise positioning of the samples, in order to enable analyses of the same surfaces at different times (Fig. 1).

Firstly, rectangular pieces of yellow adhesive tape (4 × 5 mm) were attached at the middle third of the labial surfaces of the teeth, corresponding to the bracket bonding area. The external borders of the adhesive tapes were used as reference points for sectioning the crowns from the buccal to the lingual face, in the mesiodistal and gingivo-occusal direction, using diamond discs (Type 7012, KG Sorensen, Cotia, São Paulo, Brazil) at low speed. To ensure the integrity of the specimen, the total thickness of the enamel and dentin was completely preserved (in-depth) as both the buccal and lingual faces of the crowns were well conserved. The samples were then reanalyzed to be selected by the same criteria for tooth selection, and excluded if necessary, when observing damages caused by the preparation (sectioning) process, by using an optical microscope (Model L2000A; Bioval, São Paulo, SP, Brazil) at ×20 on scope magnification.

The tooth segment samples were fitted into plastic screw cover caps containing a small piece of red wax, keeping the labial portions exposed upwards. The caps were then glued onto the centers of perfectly square aluminum bases ($25 \times 25 \times 2.5\ mm^3$) using Loctite Universal Super Glue (Henkel Corporation, Rocky Hill, CT, USA). A silicone mold was used as a template to guide the positioning of the caps over the aluminum bases. The enamel samples were subsequently embedded in the plastic caps with self-curing acrylic resin (Duralay, Reliance Dental Co., Worth, Illinois, USA). In order to ensure precision of the analyses performed at different times, a perforation was made on the left border of the caps, using a number 5 dental explorer. The site for the perforation was guided by a line marked with an overhead projector pen on the left edge of the silicone mold. The perforation (denoted point 0) was used as a reference for the starting point of the measurements. Additionally, a square window made of yellow adhesive tape was positioned on the borders of the enamel samples, in order to enable evaluation and comparison of the mesiodistal profiles of the same treated and untreated surfaces. These windows were also used to delimit and define the total enamel surface area for bracket bonding.

Clean-Up and Initial Analysis of the Enamel Surface

The tooth samples were firstly cleaned for 20 s using a low-speed rubber cup with nonfluoride pumice and water, followed by rinsing for 10 s and air-drying with gentle jets of oil-free compressed air. Initial analyses were then performed using a confocal laser scanning microscope (LEXT OLS4100, Olympus Corp., Tokyo, Japan), based on noncontact laser scanning interferometry, operating on scanning mode XYZ fast scan, with an MPLAPONLEXT 5 lens using a 1X zoom.

Bonding Procedures

The bonding procedures were performed according to the manufacturer's instructions. The uncovered enamel areas were firstly

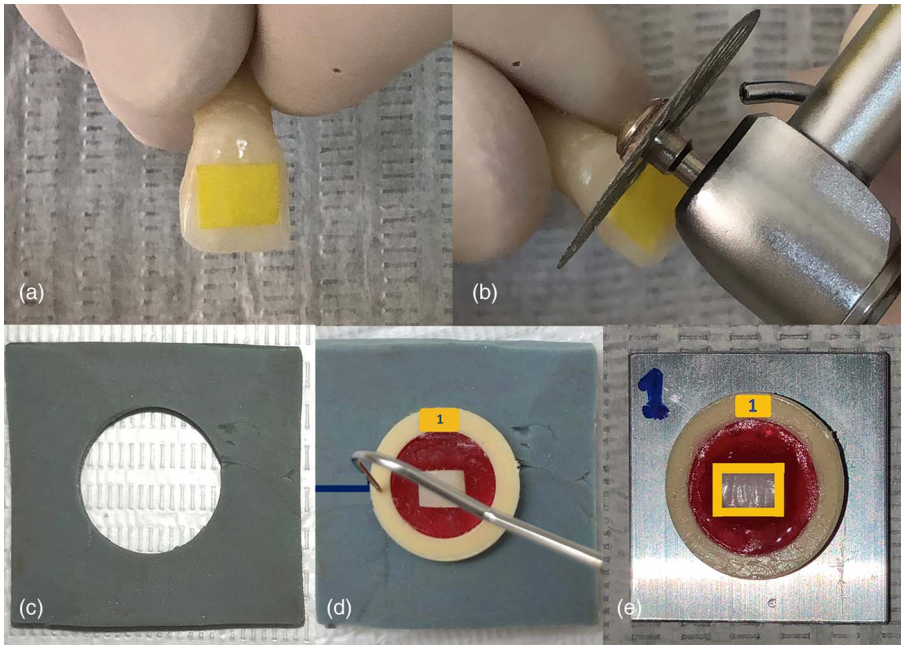

Fig. 1. Sample preparation. (**a**) Delimitation of sample size for sectioning; (**b**) sample sectioning; (**c**) silicone mold template with a circle window to guide the positioning of the caps over the aluminum bases; (**d**) accurate sample positioning using the silicone mold template; perforation to obtain the reference starting point on the left border of the caps, according to the line marked on the silicone mold; (**e**) sample prepared and positioned; yellow tape window applied over the dental surface, delimiting the bracket bonding area.

etched for 15 s with 37% phosphoric acid gel (Dentsply, Petrópolis, Rio de Janeiro, Brazil), rinsed with water for 10 s, and dried using a gentle jet of oil-free compressed air. A thin coat of adhesive primer (Transbond XT Primer Adhesive, 3 M Unitek, Monrovia, California, USA) was subsequently applied on the uncovered enamel surface areas. Ceramic brackets for maxillary central incisors (Clarity Advanced, 3 M, Monrovia, California, USA), with 0.022×0.028 inch slots and 11.6 mm^2 base surface area, were then bonded to the enamel surfaces using a light-curing orthodontic resin (Transbond XT, 3 M Unitek, Monrovia, California, USA), according to the manufacturer's recommendations. Following the bonding protocol, the brackets filled with orthodontic resin were pressed firmly for seating on the enamel surface. This technique was used to ensure ideal bond strength (ISO/TS 11405:2003) and to provide a low amount of resin remnants to be removed after debonding. The excess resin was removed using a dental explorer probe. The light-curing procedure was then performed for 10 s straight through the bracket, using a dental light-curing device (Poly Wireless, KaVo Kerr, Joinville, SC, Brazil), following its manufacturer's recommendations for bonding ceramic brackets. After bonding, the samples were stored in purified water for 24 h at 37°C to ensure complete polymerization of the adhesive before the debonding procedures.

Bracket Debonding and Finishing of the Surfaces

The brackets were debonded by first fixing the sample in a bench vice and then using the bracket debonding instrument recommended by the manufacturer (Type 804-170, 3 M Unitek, Monrovia, California, USA) and following the instructions, positioning the pliers to gently squeeze together the mesial and distal bracket wings until they peeled away from the enamel sample. The removal of all visible residual resin was performed using an orthodontic polishing system (American Burrs, Palhoça, Santa Catarina, Brazil). Firstly, remnants of materials were removed from the enamel surfaces using ultra-green coarse-grained followed by ultra-white fine-grained Arkansas stones. Polishing was then performed using a sequence of wheel-shaped gray coarse-grained and fine-grained ultra-gloss resin polishers. All procedures were performed at low speed and with cooling under water.

Three-Dimensional Evaluation of Enamel Surfaces

The enamel surfaces were measured and analyzed before and after debonding followed by the finishing procedure, using the Olympus LEXT OLS 4100 noncontact 3D confocal laser scanning digital microscope.

To ensure analysis at different trial times, the samples on aluminum bases were firstly fitted into two inner sides (forming an angle of 90°) of a plastic set-square previously attached to the motorized table of the microscope. The evaluation areas in the central portions of the enamel samples were defined by first positioning the autofocus lenses of the equipment over the starting reference point 0 (Fig. 2a). The image of the perforation on the computer screen was positioned superimposed on the intersection point of the x (red line) and y (green line) coordinates, provided by the software of the equipment, indicated by the white arrow in Figure 2b. The numerical values of the x and y coordinates were then recorded in order to ensure correct repositioning of the specimen. Both the intersection point of the x and y coordinates and the point 0 had to be coincident in order to ensure the precise repositioning of the samples at different times. Figure 2c shows the image of the perforation on the computer screen (indicated by the white arrow), representing the point 0. From the point 0, the motorized table was moved 8 mm transversally, in the mesiodistal direction, for measuring the reading area in the center of the

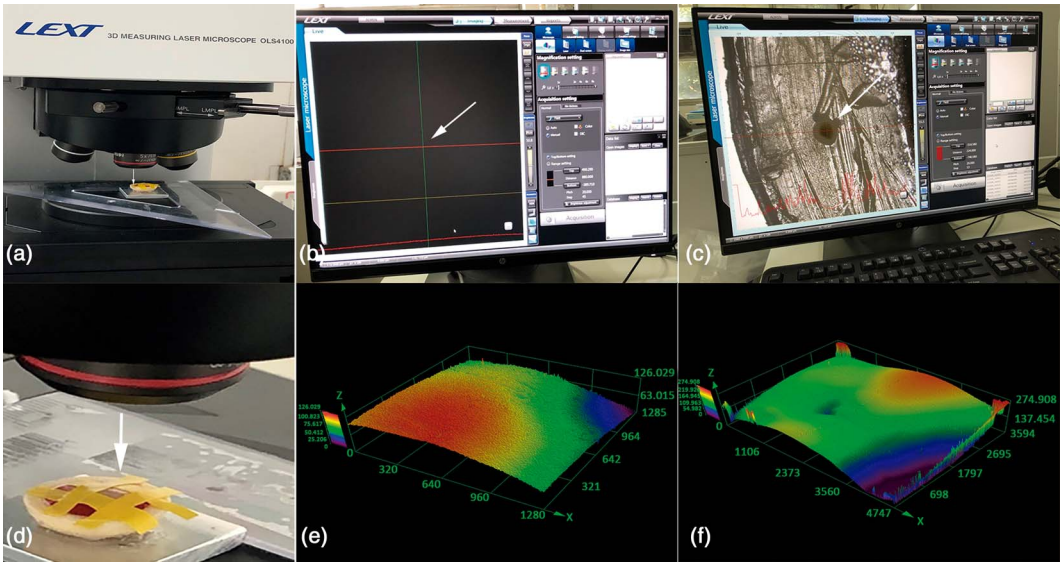

Fig. 2. Three-dimensional measuring and analysis process (a detailed description of the procedure is provided in the text).

enamel sample (Fig. 2d). The measurements were firstly performed in an area of 1,280 × 1,280 μm^2, followed by a panoramic assessment of the entire bonding area. The three-dimensional high-resolution characterization of both areas are shown, respectively, in the images displayed on Figures 2e and 2f.

Quantitative Analysis

The enamel surfaces were assessed to quantify their roughness and the loss of enamel at different times of the trial, with the determination of three amplitude parameters:

- Average roughness value (Sa), corresponding to the arithmetic mean of the heights of peaks and depths of valleys, starting from a mean line.
- Root mean square roughness (Sq), corresponding to the height distribution relative to the mean line.
- Peak to valley height (Sz) over a measurement on the profile (ISO 25178-2).

In addition, a grid template was constructed for comparison of the three-dimensional images of the enamel surfaces before and after treatment, generated by the equipment software.

Color scale and gray scale maps were used to represent surface topographical features, semi-quantitatively analyzed by the equipment software. The colorimetric scale map represents the data points obtained for the surface in the vertical *z*-axis, with (ordered from the top to the bottom) red and light red colors describing the highest peaks, yellow and green showing the intermediate points of the surface, and dark blue and magenta indicating the deepest valleys (deepest points of the surface). Otherwise, the gray scale describes a range of shades of gray, with the whiter parts denoting features on the top of the surfaces and the black colors showing cavities in the surfaces.

Results

Comparison of the images acquired at the start (T0) and end (T1) of the procedure confirmed that the positioning could be repeated with high precision. The superimposition of the inner portions of the grid template over the images of the same 1,280 × 1,280 μm^2 area of enamel sample 1, acquired before and after treatment, showed that the precision of the 3D measurements was satisfactory (Fig. 3).

Specific characteristics such as waviness, erosion, scratches, and enamel microcracks in small areas and in the entire field representing the bracket bonding area could be reproduced, compared, and analyzed before and after testing. Figure 4 shows the three-dimensional characterization of sample 2. The surface analysis of an area measuring 1,280 × 1,280 μm^2 before treatment (Figs. 4a, 4c, using colorimetric and gray scales) showed the presence of erosion and scratches (indicated by the white arrows). After the treatment (Figs. 4b, 4d), there was a reduction of roughness, increased wear (vertical loss) on the surface, and the presence of small remnant fragments of resin (Fig. 4b), as well as the appearance of small erosion sites (shown by the white arrows in Fig. 4d).

Figure 5 shows panoramic images of sample 3 (using colorimetric and gray scales) for assessment of the entire bonding area before (Figs. 5a, 5c) and after treatment (Figs. 5b, 5d), revealing surface features including erosion, microcracks, and waviness. The mesiodistal profiles (corresponding to the orange lines shown in the upper sections of Figs. 5c, 5d) of the sample before and after treatment are shown in the lower sections of Figures 5c and 5d.

Quantitative analysis of the surfaces of the samples at different stages of the trial enabled the evaluation of surface alterations, such as roughness and wear, after the treatment (Fig. 6).

Discussion

The literature indicates that debonding procedures can cause irreversible damage to enamel surfaces (Eminkahyagil et al., 2006). Debonding of ceramic brackets is not considered safe, due to the risk of enamel damage caused by the higher bonding strength of the ceramic bracket base, compared to that of a metal bracket, and the bonding systems that have been developed to increase the

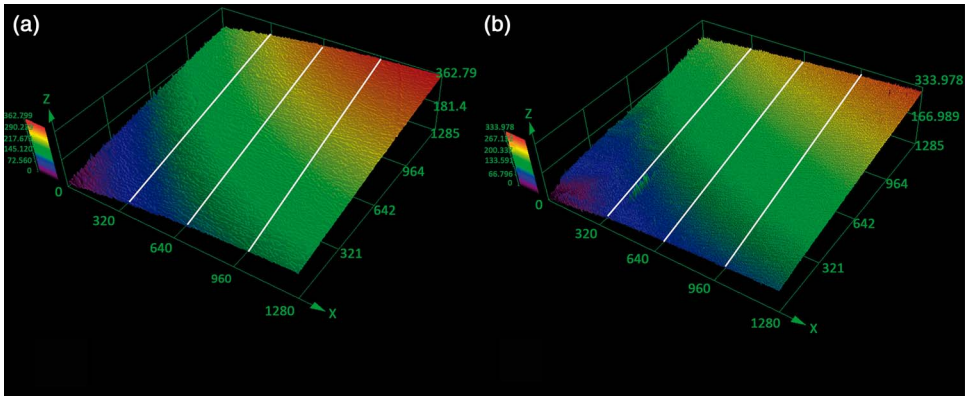

Fig. 3. Evaluation of the precision of the 3D measurements performed for sample 1, on the same dental enamel surface area, (**a**) before bonding (baseline) and (**b**) after debonding followed by resin removal and finishing. The reduction of light red areas and the increase of dark blue areas show the increased wear on the surface after the treatment.

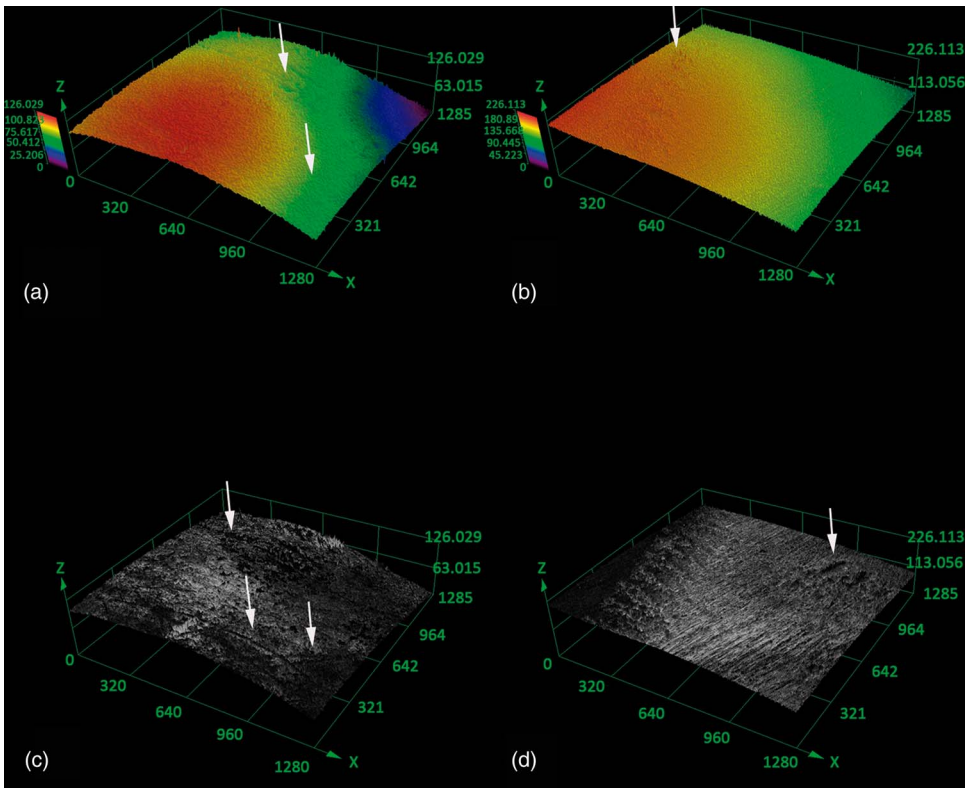

Fig. 4. Three-dimensional surface analysis of an area measuring 1,280 × 1,280 μm^2 on sample 2 before (**a,c**) and after (**b,d**) treatment. A description of the observed features is provided in the text.

strength of bonds involving the enamel, the adhesive, and the bracket (Gwinnett, 1988; Bishara et al., 2002). Damage can occur because high bond strength values may exceed the cohesive strength of the enamel, favoring the appearance of cracks and fractures (Rix et al., 2001). The loss of enamel after bracket removal may be clinically significant, especially if it occurs in the outer layer of the enamel, which contains a high percentage of minerals and the highest concentration of fluoride (which declines after the first 20 μm of the uppermost surface layer of the tissue) (Brown & Way, 1978). Therefore, damage to the substrate may lead to decreased resistance of the enamel, increasing the risk of demineralization (Øgaard et al., 2001; Karan et al., 2010). Another aspect to be highlighted is the existence of resin remnants, as revealed in the present study, even after resin removal by the finishing procedures. These fragments could facilitate the formation of decalcified areas and caries lesions, in addition to causing surface discoloration and negatively impacting dental esthetics, which is an extremely important factor in orthodontic treatments (Gwinnett & Ceen, 1979).

In order to increase analytical reliability, it has been suggested that after debonding and polishing, the previously bonded areas of the enamel should be compared to adjacent nontreated surfaces of the same specimens (Pignatta et al., 2012). In the present pilot study, the new method for sample evaluation was able to provide

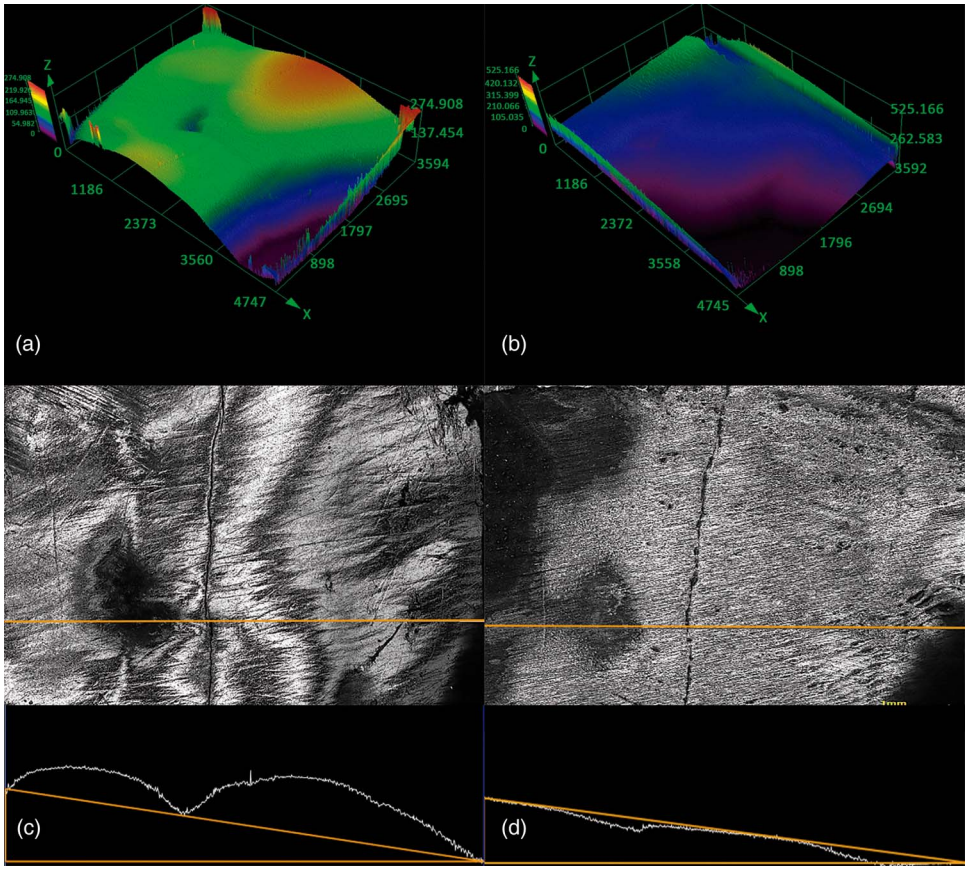

Fig. 5. Panoramic images of sample 3 for assessment of the entire bonding area before (**a,c**) and after treatment (**b,d**). A description of the observed features is provided in the text.

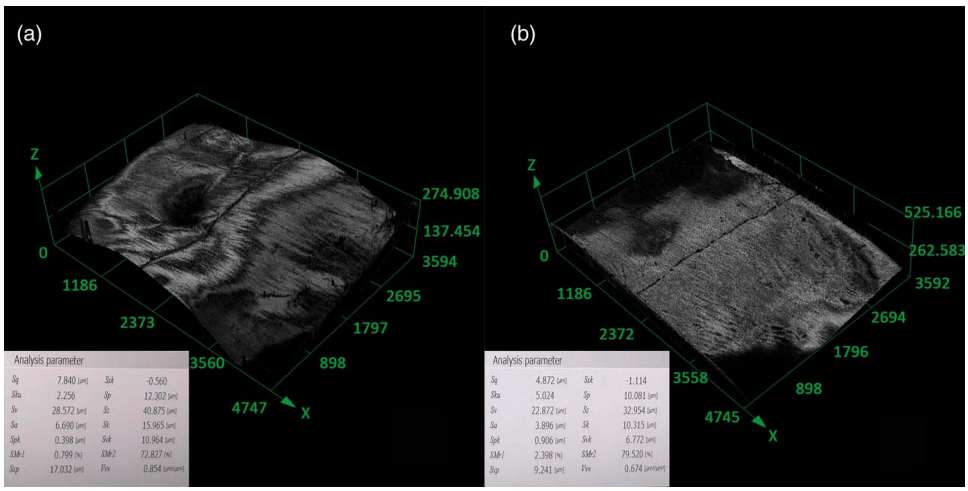

Fig. 6. Quantitative analyses before (**a**) and after (**b**) treatment, showing decreased roughness (parameters Sa and Sq) and increased wear (lower value for parameter Sz) post-treatment.

the characterization of features on enamel surfaces, before and after ceramic bracket debonding and surface finishing procedures. According to its manufacturer specifications sheet, the three-dimensional noncontact laser scanning microscope technique employed here enables rapid high-definition image acquisition and observation under a horizontal (X–Y direction) resolution of 0.12 μm, and a 10-nanometer resolution, in the Z-axis direction, to permit high-resolution 3D surface contour measurement. A precise 0.8 nanometer-resolution linear scale and software algorithms can resolve height differences of 10 nanometers with an automatic line stitching function for profile measurement for sample lengths up to 100 mm. The operational capabilities permit nanometric analysis of characteristics such as roughness and wear, regardless of surface texture conditions, on nonflat

(uneven) surfaces, whether they are curved (concave or convex), with steps or even sloped up to 85°, of samples with multiple layers, measuring the thickness of each layer individually.

The measuring tool provides high accuracy (which indicates how close a measurement is to the true value) and high repeatability (which indicates the degree of variation among the values obtained in repeated measurements). The novel methodology allows successive qualitative and quantitative analyses and comparisons of the entire topographic structure or of specific characteristics on large or small areas of the same enamel surfaces, under different testing conditions.

Several qualitative and quantitative methods have been used to diagnose alterations on enamel surfaces subjected to ceramic bracket bonding, including SEM, optical stereomicroscopy (with or without a digital camera), a magnifying lens (10×) and transillumination with a fiber optic light head, and 3D OCT scanning (Ahrari et al., 2012; Kitahara-Céia et al., 2008; Bishara et al., 2008; Dumbryte et al., 2015, 2017; Janiszewska-Olszowska et al., 2015; Leão Filho et al., 2015; Machoy et al., 2019). To date, SEM has been the method most widely used for the evaluation of enamel quality after ceramic bracket debonding. However, SEM typically requires gold coating of the sample surface before analysis, which hinders detection of major surface lesions or irregularities (Kitahara-Céia et al., 2008). Consequently, the evaluation of enamel surfaces using SEM micrographs can be subjective and unreliable (Karan et al., 2010). Furthermore, as the surfaces cannot be quantitatively evaluated, this method is not entirely suitable for comparative assessments of enamel roughness (Fjeld & Øgaard, 2006; Field et al., 2010).

Elsewhere, it was suggested that the distinction between the loss of enamel and residual resin could be investigated by three-dimensional analysis using noncontact laser scanning techniques (Al Shamsi et al., 2007). Alternatively, OCT has been considered as a potential noninvasive method for the diagnosis of enamel damage, permitting measurement of the entire thickness of the enamel layer, before and after ceramic bracket debonding (Leão Filho et al., 2015; Machoy et al., 2019). However, no OCT protocol has yet been published providing comparisons for the same specific areas or surface points, showing the presence of injuries on the tooth enamel that could influence the final surface topography obtained after debonding procedures. Furthermore, mapping of the surface topography does not seem to be feasible using this technique.

Irrespective of the methodology used in three-dimensional techniques, no previous studies presented a protocol for ensuring a high level of repeatability in investigations of the same surface sites, which is required for the accurate description of roughness and wear patterns after different test conditions. Therefore, it was not possible to determine how specific surface characteristics observed before testing, such as grooves, microcracks, waviness, or erosion, could have evolved and affected the features of the same whole surface after different test conditions. Consequently, mapping of the surface topography of ceramic bracket bonded areas could be unfeasible, or the results could be misleading.

To date, although some studies using noncontact three-dimensional technologies have aimed at the evaluation of enamel before and after debonding of ceramic brackets (Leão Filho et al., 2015; Suliman et al., 2015; Machoy et al., 2019), the proposed techniques have shown limitations in terms of the ability to perform repeated quantitative assessments of surface characteristics, preventing the analysis and interpretation of reliable data. Therefore, the aim of the present pilot study was to establish a systematic protocol enabling accurate successive qualitative and quantitative evaluations of specific enamel surface alterations during different test conditions.

The results showed that the novel technique developed here can be used as a powerful tool for the noncontact 3D evaluation of micrometric surface characteristics such as roughness, wear, erosion, and microcracks, using images acquired at the nanometric scale. This new methodology makes it possible to correlate data for the same enamel surface of the entire ceramic bracket bonded area, before and after debonding, with full noncontact 3D characterization of the surface. The wider adoption of this technique could lead to advances in understanding the effects of debonding of ceramic brackets on human tooth enamel.

Conclusions

The new protocol using confocal laser scanning microscopy provided qualitative and quantitative assessment of changes on the same dental surfaces at different trial times. The advantages of this methodology indicate its suitability for wider usage aiming at understanding problems related to orthodontic ceramic appliance debonding. It can contribute to clinical safety by elucidating the causes of minor damage to the enamel surface and evaluating the clinical feasibility of the chosen debonding procedure. The protocol is presented as a validated tool for determining and correlating the effects of debonding of ceramic brackets on sound or previously injured dental enamel surfaces.

Acknowledgments. Special thanks are due to José Maria Suhett de Azevedo (Labiom-R) for his assistance in the microscopy evaluations.

Conflict of interest. The authors declare that they have no conflict of interest.

References

Ahrari F, Heravi F, Fekrazad R, Farzanegan F & Nakhaei S (2012). Does ultra-pulse CO_2 laser reduce the risk of enamel damage during debonding of ceramic brackets? *Lasers Med Sci* **27**, 567–574.

Al Shamsi AH, Cunningham JL, Lamey PJ & Lynch E (2007). Three-dimensional measurement of residual adhesive and enamel loss on teeth after debonding of orthodontic brackets: An in-vitro study. *Am J Orthod Dentofacial Orthop* **131**(301), e9–e15.

Bishara SE, Laffoon JF, VonWald L & Warren JJ (2002). The effect of repeated bonding on the shear bond strength of different orthodontic adhesives. *Am J Orthod Dentofacial Orthop* **121**, 521–525.

Bishara SE, Ostby AW, Laffoon J & Warren JJ (2008). Enamel cracks and ceramic bracket failure during debonding in vitro. *Angle Orthod* **78**, 1078–1083.

Brown CRL & Way DC (1978). Enamel loss during orthodontic bonding and subsequent loss during removal of filled and unfilled adhesives. *Am J Orthod* **74**, 663–671.

Campbell PM (1995). Enamel surfaces after orthodontic bracket debonding. *Angle Orthod* **65**, 103–110.

Cochrane NJ, Lo TWG, Adams GG & Schneider PM (2017). Quantitative analysis of enamel on debonded orthodontic brackets. *Am J Orthod Dentofacial Orthop* **152**, 312–319.

Dumbryte I, Jonavicius T, Linkeviciene L, Linkevicius T, Peciuliene V & Malinauskas M (2015). Enamel cracks evaluation – A method to predict tooth surface damage during the debonding. *Dent Mater J* **34**, 828–834.

Dumbryte I, Jonavicius T, Linkeviciene L, Linkevicius T, Peciuliene V & Malinauskas M (2016). The prognostic value of visually assessing enamel microcracks: Do debonding and adhesive removal contribute to their increase? *Angle Orthod* **86**, 437–447.

Dumbryte I, Linkeviciene L, Linkevicius T & Malinauskas M (2017). Enamel microcracks in terms of orthodontic treatment: A novel method for their detection and evaluation. *Dent Mater J* **36**, 438–446.

Dumbryte I, Vebriene J, Linkeviciene L & Malinauskas M (2018). Enamel microcracks in the form of tooth damage during orthodontic debonding: A systematic review and meta-analysis of in vitro studies. *Eur J Orthod* **30**, 636–648.

Eminkahyagil N, Arman A, Çetinşahin A & Karabulut E (2006). Effect of resin-removal methods on enamel and shear bond strength of rebonded brackets. *Angle Orthod* **76**, 314–321.

Ferreira FG, Nouer DF, Silva NP, Garbui IU, Correr-Sobrinho L & Nouer PRA (2014). Qualitative and quantitative evaluation of human dental enamel after bracket debonding: A noncontact three-dimensional optical profilometry analysis. *Clin Oral Investig* **18**, 1853–1864.

Field J, Waterhouse P & German M (2010). Quantifying and qualifying surface changes on dental hard tissues in vitro. *J Dent* **38**, 182–190.

Fjeld M & Øgaard B (2006). Scanning electron microscopic evaluation of enamel surfaces exposed to 3 orthodontic bonding systems. *Am J Orthod Dentofacial Orthop* **130**, 575–581.

Gutiérrez-Salazar MdP & Reyes-Gasga J (2003). Microhardness and chemical composition of human tooth. *Mater Res* **6**, 367–373.

Gwinnett AJ & Ceen RF (1979). Plaque distribution on bonded brackets: A scanning microscope study. *Am J Orthod* **75**, 667–677.

Gwinnett JA (1988). A comparison of shear bond strengths of metal and ceramic brackets. *Am J Orthod Dentofacial Orthop* **93**, 346–348.

Habibi M, Nik TH & Hooshmand T (2007). Comparison of debonding characteristics of metal and ceramic orthodontic brackets to enamel: An in-vitro study. *Am J Orthod Dentofacial Orthop* **132**, 675–679.

Heravi F, Rashed R & Leila Raziee L (2008). The effects of bracket removal on enamel. *Aust Orthod J* **24**, 110–115.

Janiszewska-Olszowska J, Tandecka K, Szatkiewicz T, Stępień P, Sporniak-Tutak K & Grocholewicz K (2015). Three-dimensional analysis of enamel surfacealteration resulting from orthodontic clean-up – Comparison of three different tools. *BMC Oral Health* **15**(1), 146.

Karan S, Kircelli BH & Tasdelen B (2010). Enamel surface roughness after debonding. *Angle Orthod* **80**, 1081–1088.

Kitahara-Céia FMF, Mucha JN & dos Santos PAM (2008). Assessment of enamel damage after removal of ceramic brackets. *Am J Orthod Dentofacial Orthop* **134**, 548–555.

Leão Filho JCB, Braz AKS, de Araujo RE, Tanaka OM & Pithon MM (2015). Enamel quality after debonding: Evaluation by optical coherence tomography. *Braz Dent J* **26**, 384–389.

Machoy ME, Koprowski R, Szyszka-Sommerfeld L, Safranow K, Gedrange T & Woźniak K (2019). Optical coherence tomography as a non-invasive method of enamel thickness diagnosis after orthodontic treatment by 3 different types of brackets. *Adv Clin Exp Med* **28**, 211–218.

Øgaard B, Larsson E, Henriksson T, Birkhed D & Bishara SE (2001). Effects of combined application of antimicrobial and fluoride varnishes in orthodontic patients. *Am J Orthod Dentofacial Orthop* **120**, 28–35.

Pignatta LMB, Duarte Júnior S & Santos ECA (2012). Evaluation of enamel surface after bracket debonding and polishing. *Dental Press J Orthod* **17**, 77–84.

Powers JM, Kim HB & Turner DS (1997). Orthodontic adhesives and bond strength testing. *Semin Orthod* **3**, 147–156.

Reynolds IR (1975). A review of direct orthodontic bonding. *Br J Orthod* **2**, 171–178.

Rix D, Foley TF & Mamandras A (2001). Comparison of bond strength of three adhesives: Composite resin, hybrid GIC, and glass-filled GIC. *Am J Orthod Dentofacial Orthop* **119**, 36–42.

Suliman SN, Trojan TM, Tantbirojn D & Versluis A (2015). Enamel loss following ceramic bracket debonding: A quantitative analysis in vitro. *Angle Orthod* **85**, 651–656.